Detecting Population III stars through observations of near-IR cosmic infrared background anisotropies.

A. Kashlinsky[1,a,*], R.Arendt[1,a], Jonathan P. Gardner[2,b], J. Mather[1,b],S. Harvey Moseley[1,b]

[1]Laboratory for Astronomy and Solar Physics, Code 685, Goddard Space Flight Center, Greenbelt MD 20771

[2]Laboratory for Astronomy and Solar Physics, Code 681, Goddard Space Flight Center, Greenbelt MD 20771

[a]SSAI, [b] NASA

[*]To whom correspondence should be addressed; E-mail: kashlinsky@stars.gsfc.nasa.gov

Received _____; accepted _____

ABSTRACT

Following the successful mapping of the last scattering surface by WMAP and balloon experiments, the epoch of the first stars, when Population III stars formed, is emerging as the next cosmological frontier. It is not clear what these stars' properties were, when they formed or how long their era lasted before leading to the stars and galaxies we see today. We show that these questions can be answered with the current and future measurements of the near-IR cosmic infrared background (CIB). Theoretical arguments suggest that Population III stars were very massive and short-lived stars that formed at $z \sim 10 - 20$ at rare peaks of the density field in the cold-dark-matter Universe. Because Population III stars probably formed individually in small mini-halos, they are not directly accessible to current telescopic studies. We show that these stars left a strong and measurable signature via their contribution to the CIB anisotropies for a wide range of their formation scenarios. The excess in the recently measured near-IR CIB anisotropies over that from normal galaxies can be explained by contribution from early Population III stars. These results imply that Population III were indeed very massive stars and their epoch started at $z \sim 20$ and lasted past $z \lesssim 13$. We show the importance of accurately measuring the CIB anisotropies produced by Population III with future space-based missions.

Subject headings: cosmology: theory - cosmology: observations - diffuse radiation - large scale structure of Universe

1. Introduction

The cosmic infrared background (CIB) arises from the accumulated emission of galaxy populations spanning a large range of redshifts. The earliest epoch for the production of this background occurred when star formation first began, and contributions to the CIB continue through the present epoch. The CIB is thus an integrated summary of the collective star forming events, star-burst activity, and other luminous events in cosmic history to the present time.

With the WMAP measurements (Bennett et al 2003) the structure of the last scattering surface has been mapped and a firm cosmological model has now emerged: the Universe is flat, dominated by the vacuum energy or an exotic quintessence field and is consistent with the inflationary paradigm and a cold-dark-matter (CDM) model. In this paper, we adopt the ΛCDM model with cosmological parameters from the WMAP and other observations: $\Omega_{\rm baryon} = 0.044, h = 0.71, \Omega_{\rm m} = 0.3, \Omega_\Lambda = 0.7, \sigma_8 = 0.84$. Following the last scattering at $z \sim 1000$, the Universe entered an era known as the "Dark Ages", which ended with the star formation which produced Population III stars. The WMAP polarization results (Kogut et al 2003) show that the Universe had an optical depth since last scattering of $\tau \sim 0.2$, indicating an unexpectedly early epoch of the first star formation ($z_* \sim 20$). From the opposite direction in z, optical and IR telescopes are now making progress into understanding the luminosity history during the most recent epoch of the universe ($z < 5$), but the period from recombination to the redshift of the galaxies in the Hubble Deep Field (HDF) remains largely an unexplored era. The first objects in the Universe probably formed in mini-halos of $\sim 10^{5-6} M_\odot$ (e.g. Miralda-Escude 2003) (barring the possible radiative feedback effects), which would remain largely inaccessible to current instruments and conventional methods.

A consensus based on recent numerical investigations is now emerging that fragmentation of the first collapsing clouds at redshift z_* was very inefficient so that the first metal-free stars were extremely massive with mass $\gtrsim 100 M_\odot$ (Abel et al 2002, Bromm et al 1999). Such stars would live only a few million years, which is much less than the age of the Universe ($\simeq 2 \times 10^8$ years

at $z = 20$), making their direct detection still more difficult. It is unclear how long the era of Population III stars lasted and when the Population II stars formed with metallicities $\sim 10^{-3}$ solar (Schneider et al 2002). On the other hand the net radiation produced by these massive stars will give substantial contributions to the total diffuse background light (Rees 1978) and since their light is red-shifted much of that contribution will be today in the infrared bands (Bond et al 1986) contributing significantly to the near-IR CIB.

Observationally, the CIB is difficult to distinguish from the generally brighter foregrounds from the local matter within the Solar system, and the stars and ISM of the Galaxy. A number of investigations have attempted to extract the isotropic component (mean level) of the CIB from ground- and satellite-based data (see Hauser & Dwek 2001 for a recent review). These analyses of the *COBE* data have revealed the CIB at far-IR wavelengths $\lambda > 100\mu$m(Hauser et al 1998), and probably at near-IR wavelengths from 1 - 3 μm (Dwek & Arendt 1998, Gorjian et al 2001, Cambresy et al 2001) with additional support from analysis of data from *IRTS* (Matsumoto et al 2000). However, none of the reported detections of the isotropic CIB are very robust (especially at near–IR wavelengths), because all are dominated by the systematic uncertainties associated with the modeling and removal of the strong foreground emission. Furthermore, the near-IR colors of the mean CIB do not differ greatly from those of the foregrounds, limiting the use of spectral information in distinguishing the true CIB from residual Galactic or solar system emission. Because of the difficulty of exactly accounting for the contributions of these bright foregrounds when measuring the CIB directly, and the difficulty in detecting *all* the contributing sources individually, it was proposed to measure the structure or anisotropy of the CIB via its angular power spectrum (Kashlinsky et al 1996). For a relatively conservative set of assumptions about clustering of distant galaxies, fluctuations in the brightness of the CIB have a distinct spectral and spatial signal, and these signals can be more readily discerned than the actual mean level of the CIB.

In Fig. 1, we summarize the current near-IR CIB measurements and compare the measured CIB at 1.25 and 2.2 μm to the total flux from the observed galaxy populations. There is a

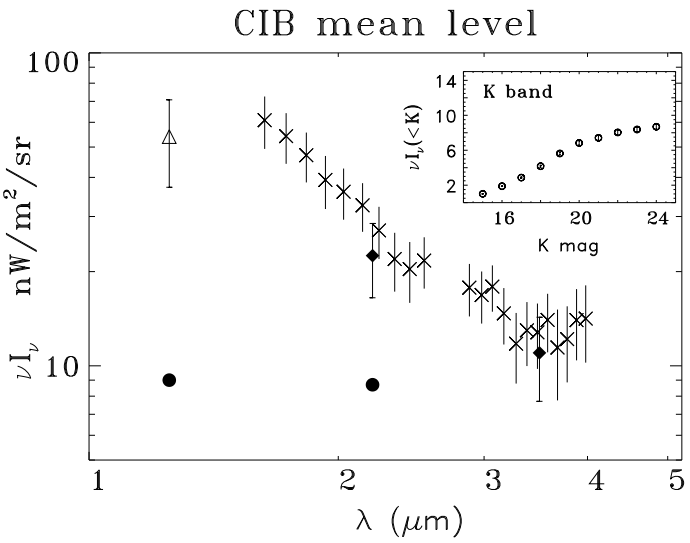

Fig. 1.— Mean levels of the near–IR CIB from IRTS (crosses from Matsumoto et al 2000 and from COBE DIRBE (filled diamonds - at 2.2 μm from Gorjian et al 2001 and at 3.5 μm from Dwek & Arendt 1998. Cumulative flux from *observed* J and K band galaxies is shown with the filled circles (Cambresy et al 2001, Gardner 1996, Kashlinsky & Odenwald 2000b) Open triangle shows the CIB results of the DIRBE J-band analysis from Cambresy et al 2001. The insert shows the cumulative flux distribution in nW/m^2/sr as a function of K magnitude from galaxies from deep galaxy surveys (Totani et al 2001).

statistically significant excess over the CIB expected from normal galaxies; e.g. at 1.25 μm (J band) and 2.2 μm (K band), while an integration of the measured galaxy counts gives only 30-40% of the observed CIB (Kashlinsky & Odenwald 2000b, Gardner 1996, Madau & Pozzetti 2000). If this deficit CIB does not come from undetected low surface brightness emission associated with local galaxies, it must come from fainter galaxies at high z.

The measurements of CIB structure or fluctuations lead to similar conclusions (Kashlinsky & Odenwald 2000a, Matsumoto et al 2000, Kashlinsky et al 2002, Odenwald et al 2003). The detection of CIB fluctuations at $\sim 0.7^o$ from COBE DIRBE bands at 1.25 to 5 micron (Kashlinsky & Odenwald 2000a) shows a signal $\sim 2-3$ times that expected from normal galaxy populations evolving via a present day IMF with the observed star formation rates out to $z \sim 3-4$ (Jimenez & Kashlinsky 1999). Recently, using combined 2MASS calibration data with long net exposures, it became possible to remove resolved galaxies and measure the near-IR CIB fluctuations spectrum from a few arcsec to a few arcmin. We argued that this signal originated from faint galaxies

(K$\gtrsim$19) at high z (Kashlinsky et al 2002, Odenwald et al 2003), and is significantly larger that what is expected from normal galaxy populations. This suggests that the excess originates from still earlier epochs.

2. CIB flux and Population III

The near-IR CIB signals detected in the 2MASS long integration data (Kashlinsky et al 2002, Odenwald et al 2003) could come from the Population III stars (Magliochetti et al 2003, Kashlinsky et al 1999, Cooray, A. et al 2003, Santos et al 2002, Salvaterra & Ferrara 2003). The argument can be generalized and shown to be nearly model-independent provided Population III stars were very massive.

Massive, metal-free stars will be dominated by radiation pressure and would radiate close to the Eddington limit: $L \simeq L_{\rm Edd} = \frac{4\pi G m_p c}{\sigma_T} M \simeq 1.3 \times 10^{38} M/M_\odot$ erg/sec, where σ_T is the cross section due to electron (Thompson) scattering. The energy spectrum for emission from these stars will be nearly featureless and close to that of a black body at $T \sim 10^{4.8-5}$K (Schaerer 2002, Tumlinson et al 2003). Unlike stars with higher metallicity, Population III stars are not expected to have significant mass-loss during their lifetime (Baraffe et al 2001). If sufficiently massive ($\gtrsim 240 M_\odot$, see Bond et al 1984) such stars would also avoid SN explosions and collapse directly to black holes. In this case their numbers could significantly exceed the minimum that would be required to produce the metallicities observed in Population II stars. The lifetime of these stars will be independent of mass: $t_L \simeq \epsilon M c^2/L \simeq 3 \times 10^6$ years, where $\epsilon = 0.007$ is the efficiency of the hydrogen burning. These numbers are in good agreement with detailed computations (Schaerer 2002).

For a flat Universe the co-moving volume per unit solid angle contained in the cosmic time interval dt is $dV = c(1+z)^{-1} d_L^2 dt$, where d_L is the luminosity distance. The flux per unit frequency interval from each of the Population III stars will be $L b_{\nu'}(1+z)/4\pi d_L^2$, where b_ν is the fraction of the total energy spectrum emitted per unit frequency and $\nu' = \nu(1+z)$ is the

rest-frame frequency. (The Population III SED is normalized so that $\int b_\nu d\nu = 1$). The co-moving mass density in these stars is $\int Mn(M,t)dM = \Omega_{\rm baryon}\frac{3H_0^2}{8\pi G}f_*$, where f_* is the fraction of the total baryonic mass in the Universe locked in Population III stars at time t. The net flux per unit frequency from a population of such stars with mass function $n(M)dM$ is given by:

$$\frac{d}{dt}I_\nu = \frac{\int Ln(M,t)dM}{4\pi d_L^2}\,(1+z)\,\langle b_{\nu'}\rangle\,\frac{dV}{dt} = \frac{c}{4\pi}\langle b_{\nu'}\rangle\langle\frac{L}{M}\rangle f_*\rho_{\rm baryonic} \qquad (1)$$

Here $\langle b_\nu\rangle \equiv \int Ln(M,t)b_\nu dM/\int Ln(M,t)dM$ denotes the mean Population III SED averaged over their initial mass function and $\langle\frac{L}{M}\rangle \equiv \int Ln(M,t)dM/\int Mn(M,t)dM$. For a Gaussian density field $f_* \sim 5\times10^{-2} - 3\times10^{-3}$, if on average Population III formed in 2–3 sigma regions (see below). Provided that L/M = constant, this result does not depend on the details of the initial mass function of Population III stars (cf. Fig. 5 in ref. Salvaterra & Ferrara 2003). (Note that for the present day stellar populations their mass-to-light ratio depends strongly on stellar mass and $\langle\frac{L}{M}\rangle$ is much smaller than the Population III value of $4\pi Gm_pc/\sigma_T \simeq 3.3\times10^4 L_\odot/M_\odot$ leading to substantially smaller net fluxes). Assuming no significant mass loss (Baraffe et al 2001) during their lifetime t_L for Population III stars, these stars will produce CIB flux of amplitude:

$$\nu I_\nu = \frac{3}{8\pi}\,\frac{1}{4\pi R_H^2}\,\frac{c^5}{G}\,\epsilon\Omega_{\rm baryon}\frac{1}{t_L}\int f_*\langle\nu' b_{\nu'}\rangle\frac{dt}{1+z} \qquad (2)$$

Note that c^5/G is the maximal luminosity that can be achieved by gravitational processes and enters here because the nuclear burning of stars evolves in gravitational equilibrium with the (radiation) pressure. This result, eq. 2, has a simple meaning illustrating its model-independence: the cumulative bolometric flux produced is $L_{\rm max} = c^5/G \simeq 10^{26}L_\odot$ distributed over the surface of the Hubble radius, $4\pi R_H^2$, times the model-dependent dimensionless factors. The spectral distribution of the produced diffuse background will be determined by $\langle\overline{b_\nu}\rangle \equiv \int f_*(1+z)^{-1}\langle b_\nu\rangle dt/\int f_*(1+z)^{-1}dt$, which is the mean SED averaged over the first star epoch (hereafter assumed to have duration t_*). The value of $L_{\rm max}/4\pi R_H^2$ is $\simeq 3\times10^8$ nW/m^2/sr so even with small values of $\Omega_{\rm baryon}, \epsilon, f_*$, the net flux from Population III stars would be substantial. The K-band roughly coincides with the Lyman limit (912 Å) at $z_* \sim 20$ so much of the emitted flux would contribute today in the near IR bands. If there was a population of massive black

holes, as seems likely to result from Population III evolution, their accretion processes will emit radiation at a much higher efficiency of $\epsilon \sim 0.1$ (and perhaps as high as $\epsilon \sim 0.4$ very close to the event horizon). At the same time, the K-band CIB excess over the total contribution from the observed galaxy populations ($\simeq 9\mathrm{nW/m^2/sr}$ up to K~ 24), is $\simeq 10 - 15\mathrm{nW/m^2/sr}$ and can be completely accounted for by the contribution from Population III stars at high redshifts.

The first stars formed in rare regions of the density field that reached the turn-around over-density while the bulk of the matter was still in a linear regime (density contrast < 1). These regions stopped expanding and began collapsing, forming the first generation of stars if certain conditions are met. For a Gaussian density field, as required for the CDM models, this would specify the value of f_* at each time. The power spectrum of the mass distribution on large scales preserved the Harrison-Zeldovich power spectrum index ($n \simeq 1$), but on scales less than the horizon scale at the matter-radiation equality, the spectrum was modified by the different growth-rates of sub- and super-horizon modes. This led to a gradual decrease of n toward the very small scale value of $n \lesssim -2$, suppressing the small scale power and leading to late collapse and galaxy formation. In this picture, it is surprising that the the first stars started forming at $z_* = 20^{+10}_{-9}$, as indicated by the WMAP polarization measurements, but the most straightforward explanation is that the earliest stars formed out of very high peaks of the density field, leading to smaller f_*.

Assuming a spherical model for growth and collapse of density fluctuations, any density fluctuation that reached the dimensionless density contrast $\delta_{\rm col} = 1.68$ will collapse. Consequently, if σ_M is the rms fluctuation at z over a sphere containing the total mass M, then $\eta \equiv \delta_{\rm col}/\sigma_M$ measures the numbers of standard deviations for that mass to collapse at that redshift. Here, σ_M is related to the underlying power spectrum via $\sigma_M^2 = \frac{1}{2\pi^2}\int P(k;z)W(kr_M)k^2dk$ where $r_M = 1.4(M/10^{12}h^{-1}M_\odot)^{1/3}(\Omega/0.3)^{-1/3}h^{-1}\mathrm{Mpc}$ is the co-moving linear scale containing mass M, and $W(x) = (3j_1(x)/x)^2$. As they collapse, the primordial clouds will quickly heat up to their virial temperature, $T_{\rm vir}$, and only efficient cooling will enable isothermal collapse, where gas pressure is smaller than gravity (or $T < T_{\rm vir}$).

The details of what determines the collapse and formation of Population III stars are not yet clear, but molecular cooling is critical in the initial stages of metal-free collapse. Molecular cooling is effective at $T \gtrsim 400$ K (Santos et al 2002), but some simulations suggest that rotational H_2 cooling can effectively dissipate binding energy of the cloud only if $T > 2000$ K (Miralda-Escude 2003). We have evaluated the rms mass density fluctuation, σ_M, for the ΛCDM model as a function of its virial temperature, assuming a molecular weight of $\mu = 1$. The left panel of Fig. 2 shows the resulting η vs z for $T_{\rm vir} = 400$K and 2000K. For a Gaussian density field and $\eta > 1$ the value of $f_* \simeq {\rm erfc}(\eta/\sqrt{2})$. One can see that Population III stars had to form out of 2 to 3 sigma fluctuations, which for a Gaussian distribution correspond to f_* varying between $\sim 5 \times 10^{-2}$ and $\sim 3 \times 10^{-3}$. Departures from spherical symmetry would accelerate the collapse, decreasing η and increasing f_*. Because η is a decreasing function of decreasing z, and f_* is a (rapidly) increasing function of decreasing η, the average $\overline{f_*}$ will be dominated by the late times of Population III evolution.

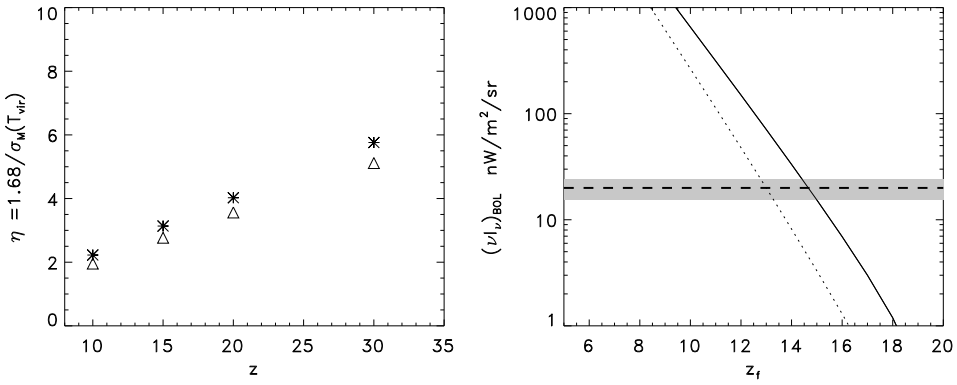

Fig. 2.— Left: The number of standard deviations that correspond to Population III regions collapsing at z for ΛCDM power spectrum of the primordial density field. Triangles correspond to $T_{\rm vir} = 400$K, asterisks to $T_{\rm vir} = 2 \times 10^3$K. Right: cumulative bolometric flux by Population III stars forming at $z_* = 20$, and lasting until z_f shown on the horizontal axis. Solid line corresponds to $T_{\rm vir} = 400$K and dotted line to $T_{\rm vir} = 2 \times 10^3$K. Thick dashed line shows the total CIB flux from DIRBE measurements at J,K and L bands; the shaded region shows the uncertainty. The values adopted were 22.9 ± 7.0 KJy/sr in J band (Cambresy et al 2001) and $16.1 \pm 4.4, 13.4 \pm 3.7$ KJy/sr in K, L bands (Wright 2003).

The right panel of Fig. 2 shows that the total diffuse background light produced during the first star era should be substantial and measurable. Much of the diffuse flux produced by the

Population III stars will today be observable in the near-IR, and could be responsible for the observed excess near-IR CIB. If z_f is large the net bolometric flux from Population III is smaller, but because of the redshift effects a larger fraction of the bolometric flux will be observed today in the near-IR bands. Furthermore, the near-IR part of the CIB emission from Population III would be increased because much of the shorter wavelengths emission gets absorbed and re-emitted at these bands by Lyman and free-free emission from the ionized nebulae around Population III stars (Santos et al 2002). Dashed line shows the total CIB flux evaluated from the DIRBE 1.25 to 3.5 μm bands. Taken at face value that would imply that the first star era lasted until $z_f \lesssim 15$. However, Population III stars only contribute a fraction of the observed CIB.

3. CIB anisotropies from Population III

The contribution of Population III stars to the CIB will possess a spatial structure that is related to that of density fluctuations from which the stars formed. At particular spatial scales and wavelengths it may prove easier to distinguish the Population III contribution from the various foregrounds through the spatial structure rather than the measurement of the mean (isotropic) intensity.

In the limit of small angles the 2-dimensional angular power spectrum, $P_2(q)$, of the CIB fluctuations that arise from clustering of Population III systems with the 3-dimensional power spectrum $P_3(k)$ is given by the modified Limber equation (Kashlinsky & Odenwald 2000a):

$$P_2(q) = \frac{1}{c}\int \left(\frac{dI_{\nu'}}{dt}\right)^2 \frac{P_3(qd_A^{-1};z)}{d_A^2} dt \qquad (3)$$

where d_A is the comoving angular diameter distance. The power spectrum P_3 is in turn related to the underlying ΛCDM model power spectrum and its evolution and growth. On larger angular scales ($\theta \gtrsim$ a few arcmin) the power spectrum is in the linear regime and we evaluate the growth rate of fluctuations using linear theory for the Λ-dominated cosmology.

On sufficiently small scales the primordial power spectrum of the density field will be modified

by non-linear gravitational effects. Fig. 3 shows the density field for the ΛCDM model at various high redshifts. The linear power spectrum was taken to be that of the ΛCDM for the WMAP cosmological parameters. The non-linear evolution of the density field was modeled analytically using the approximation from ref. (Peacock & Dodds 1996). For reference 1 arcmin subtends the comoving scale of $\sim 1.5h^{-1}$Mpc at z between 6 and 15 for WMAP cosmological parameters and a dark energy equation of state with $w = -1$. The dotted line shows the linearly evolved density field at $z = 15$. On sub-arcminute scales the density field is in the quasi-linear to non-linear regime (density contrast $\gtrsim 0.2$) for the ΛCDM model. There the spectrum due to clustering evolution was modified significantly and the fluctuations amplitude has increased from its primordial value, especially since the effective spectral index on these scales for ΛCDM model was $n \lesssim -2$.

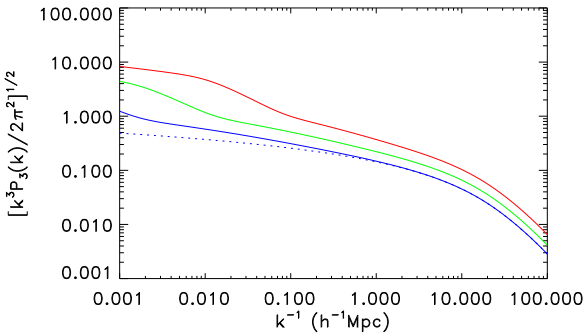

Fig. 3.— ΛCDM density field at $z = 6, 10, 15$ (red, green and blue). Dotted line corresponds to linearly evolving density field at $z = 15$.

To within a factor of order unity, the square of the fractional fluctuation of the CIB on angular scale $\simeq \pi/q$ is $\delta^2_{\rm CIB} = \langle(\delta I_\nu)^2\rangle/I^2_\nu \simeq I_\nu^{-2} q^2 P_2(q)/2\pi$. The meaning of eq. 3 can be demonstrated by assuming $dI_{\nu'}/dt$=constant during the Population III phase of duration t_*. In this case the fractional fluctuation due to clustering of early star systems becomes:

$$\delta^2_{\rm CIB} = \frac{\pi}{t_*} \int \Delta^2(q d_A^{-1}; z) dt \qquad (4)$$

Here $\Delta(k) = [\frac{1}{2\pi^2} \frac{k^2 P_3(k)}{ct_*}]^{1/2}$ is the fluctuation in number of sources within a volume $k^{-2} ct_*$. In other words, the fractional fluctuation on angular scale π/q in the CIB from Population III stars

is given by the average value of the r.m.s. fluctuation from Population III spatial clustering over a cylinder of length ct_* and diameter $\sim k^{-1}$. At $z = 20$ the Universe is $\sim 2 \times 10^8$ years old which is much larger than the age of the individual Population III stars, $t_L \sim 3 \times 10^6$ years. If the first stars lasted for only one generation forming at z_*, the relative CIB fluctuations will be $\delta_{\rm CIB} \sim \sqrt{\pi}\Delta(qd_A^{-1}; z)|_{z_*}$.

Several points are worth noting about eq. 3: Firstly, the value of $\Delta(k)$ is inversely proportional to $\sqrt{t_*}$ and thus measures the duration of the first star era. The density perturbations grow with decreasing z, so most of the contribution to the integral in eq. 3 comes from the low end of z. The overall dependence on t_* wins out and the longer the Population III phase, the smaller are the relative fluctuations of the CIB from them. Secondly, in the Harrison-Zeldovich regime of the power spectrum, $P_3 \propto k$, one would have $\delta_{\rm CIB} \propto q^{1.5}$. Finally, the transition to the Harrison-Zeldovich regime occurs in the linear regime at all relevant redshifts and happens at the co-moving scale equal to the horizon scale at the matter-radiation equality. This feature would occur at different angular scales as the redshift of the Population III era decreases. All this would allow probes of the epoch of the first stars, its duration, and the primordial power spectrum at high redshifts on scales that are currently not probed well. Interestingly, a short duration for the first stars will lead to smaller CIB flux, but larger relative fluctuations and vice versa.

In addition to the small angular scale increase due to non-linear gravitational evolution, the fluctuations in the distribution of Population III systems will be amplified because, as Fig. 2 shows, these systems had to form out of rare peaks of the primordial density field. Consequently, their 2-point correlation function will be amplified (Kaiser 1984, Jensen & Szalay 1986, Politzer & Wise 1984, Kashlinsky 1987, Kashlinsky 1998) over that given by the ΛCDM power spectrum, $\xi = \frac{1}{2\pi^2}\int P_3(k) j_0(kr) k^2 dk$. Adopting a Press-Schechter prescription for the formation of collapsed objects (Press & Schechter 1974) from a correlated density field leads to the following expression for the amplification of the 2-point correlation function (Kashlinsky 1998):

$$\xi_\eta = \xi \sum_{m=0}^{\infty} \frac{\eta^{2m}}{m!\ \delta_{\rm col}^{2m}}\ \xi^m\ \left[\frac{H_{m+1}^2(\eta/\sqrt{2})}{2\eta^2} + \frac{H_{m+2}^2(\eta/\sqrt{2})}{4(m+1)\delta_{\rm col}^2}\right] \qquad (5)$$

where H_n are Hermite polynomials. At large values of η this reduces to $\xi_\eta \simeq \exp(\eta^4\xi/\delta^2_{\rm col}) - 1$. At small values of $\xi \ll 1$ (and sufficiently large angular scales) the amplification factor is linear and equal to $\simeq \eta^4/\delta^2_{\rm col}$. At very small scales the amplification is non-linear in ξ and will exceed the linear amplification value leading to *larger* CIB fluctuations. We computed the resultant CIB fluctuations using the linear bias amplification approximation, but note that this gives a *lower* limit on the resultant CIB fluctuations.

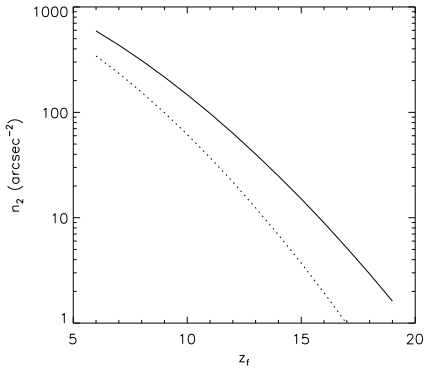

Fig. 4.— Mean projected surface density of Population III systems along the line of sight, plotted vs the redshift marking the end of the Population III era. Solid and dotted lines correspond to primordial clouds containing Population III with $T_{\rm vir} >$ 400 K and 2000 K respectively.

There will also be shot-noise fluctuations due to individual Population III systems entering the beam. The relative magnitude of these fluctuations will be $N^{-1/2}_{\rm beam}$, where $N_{\rm beam}$ is the number of the Population III systems within the beam. This component will be important at very small angular scales, where $N_{\rm beam} \sim 1$, and will contribute to the power spectrum: $P_{\rm SN} = 1/n_2$, where $n_2 = c\int n_3 d^2_L(1+z)^{-1}dt$ is the projected angular number density of Population III systems. Detection of the shot-noise component in the CIB power spectrum at small angular scales will give a direct measure of both the duration of the first star era and constrain the makeup and masses of the Population III systems. The three-dimensional number density can be evaluated from the Press-Schechter (Press & Schechter 1974) formalism, but in the appropriate limits ($\eta > 1$) it becomes $n_3 \sim \rho_{\rm baryon} M^{-1}{\rm erfc}(\eta(z)/\sqrt{2})$. Fig. 4 shows that the mean projected surface density of Population III systems n_2 for $T_{\rm vir} >$ 400 K and 2000 K. One can see that unless the Population

III era was very short, the shot noise correction to the CIB would be small on scales greater than a few arcseconds.

Essentially all of the flux emitted at rest wavelength less than 912 Å will be absorbed by the Lyman continuum absorption in the surrounding medium (Yoshii & Peterson 1994) and the contribution to the CIB will be cut off at $\lambda < 912(1 + z_f)$ Å. At longer wavelengths the flux, including emission from the nebulae around each star, will propagate without significant attenuation. Population III stars emit as black bodies at $\log T \simeq 4.8 - 5$ (Schaerer 2002) and the Lyman limit at $z \sim 20$ is shifted to $\sim 2\mu$m in the observer's frame. The 2MASS J band filter contains emission out to 1.4 μm and represents the shortest wavelength where excess in the CIB over that from normal galaxies has been measured (Cambresy et al 2001, Kashlinsky et al 2002). If the measured excesses in CIB fluctuations (Kashlinsky et al 2002, Kashlinsky & Odenwald 2000a) and isotropic component (Cambresy et al 2001) at J band are indeed attributable to Population III, their era must have lasted until $z \lesssim 14$.

Fig. 5 shows the resultant CIB fluctuations from Population III stars at 1.25, 2.2 and 3.5 micron or J, K and L photometric bands. The assumed CIB fluxes from Population III are listed near the tops of the panels. At 2.2 micron the galaxies contribute around 9 nW/m^2/sr whereas the net CIB flux is around 20-25 nW/m^2/sr ; hence the assumed excess of 10-15 nW/m^2/sr is attributed to the Population III stars for the purposes of this discussion and is taken to be 12 nW/m^2/sr in the figure. The situation is similar at 3.5 micron (Dwek & Arendt 1998, Gorjian et al 2001) and the excess was taken to be 5 nW/m^2/sr (Wright 2003). The excess in the J band over the total flux from normal galaxies was taken from (Cambresy et al 2001). The clustered component of the CIB fluctuation displayed in the figure can be rescaled to other CIB fluxes via eq. 4. Thin colored lines assume constant rate of production of the Population III fraction of the CIB and the flat SED with $b_\nu =$ constant. All Population III stars were assumed to start forming at $z_* = 20$, but different colored lines correspond to different values of z_f, the redshift of the end of the first star era. Thick colored lines correspond to a Population III contribution produced by black-body emitters in the Rayleigh-Jeans regime ($b_\nu \propto \nu^2$) with the rate of flux production $\propto f_*$.

We also computed CIB fluctuations with the rate of flux production $\propto f_*$ for more realistic SED from Santos et al (2002) which include the Lyman-α and free-free emission from the surrounding nebula. Thin and thick dashed colored lines correspond to two possible extremes: SEDs from their Fig. 3 (completely opaque nebula to ionizing photons) and Fig. 5 (completely transparent nebula). Because they do not differ significantly from the more simple SEDs the lines are shown only for some values of z_f to avoid overcrowding in the Figure. The graphs show the relative model-independence of the relative CIB fluctuations on the SED for a fixed total CIB flux; the latter contains the bulk of information on the details of Population III emission distribution between various NIR bands. For a given Population III CIB isotropic component, the fluctuations are largest for large values of z_f because the duration of the first star era is the smallest. Because of the Lyman continuum absorption there would be no appreciable CIB fluctuations at J band if $z_f \gtrsim 14$ (no blue lines in the left panel) and the contribution to the other scenarios will come from $z \sim 13$, rather than $z = 20$ when the first star era was assumed to start. This would be broadly consistent with the limits on sky brightness fluctuations at 4 μm from Xu et al (2003).

Both DIRBE and 2MASS data indicate CIB anisotropies at amplitudes larger than the contribution from normal galaxy populations (Kashlinsky & Odenwald 2000a, Kashlinsky et al 2002) and are consistent with significant contributions due to Population III. However, because the measured signal contains contributions from remaining galaxies (all galaxies for DIRBE and $K \geq 19$ galaxies for 2MASS), it is difficult to isolate the contribution from the Population III stars.

4. Prospects for measuring CIB from Population III

Population III stars, if massive, should have left a unique and measurable signature in the near-IR CIB anisotropies over angular scales from ~ 1 arcminute to several degrees as Fig. 5 shows. As is the case for measurement of the mean isotropic CIB, detection of these fluctuations depends on the identification and removal of various foreground emission (and noise) contributions:

atmosphere (for ground-based measurements), zodiacal light from the Solar system, Galactic cirrus emission, and instrument noise.

The dashed line in Fig. 5 shows the small scale atmospheric fluctuations at 2 μm after one hour of integration of ground based measurement (Odenwald et al 2003). At large angular scales atmospheric gradients will become important, making measurements there even more difficult. Atmospheric effects can be highly variable on a wide range of time scales, yet they can be completely avoided with space–based experiments. Zodiacal emission from interplanetary dust (IPD) is the brightest foreground at most IR wavelengths over most of the sky. There are some structures in this emission associated with particular asteroid families, comets, and an earth–resonant ring, but these structures tend to be confined to low ecliptic latitudes or otherwise localized. The main IPD cloud is generally modeled with a smooth density distribution. Observationally, intensity fluctuations of the main IPD cloud have been limited to $< 0.2\%$ at 25 μm (Abraham et al 1997). Extrapolating this limit to other wavelengths using the mean high–latitude zodiacal light spectrum yields the limits shown in Figure 5. Because the Earth is moving with respect to (i.e. orbiting within) the IPD cloud, the zodiacal light varies over time. Likewise, any zodiacal light fluctuations will not remain fixed in celestial coordinates. Therefore repeated observations of a field on timescales of weeks to months should be able to distinguish and reject any zodiacal light fluctuations from the invariant Galactic and CIB fluctuations.

Intensity fluctuations of the Galactic foregrounds are perhaps the most difficult to distinguish from those of the CIB. Stellar emission may exhibit structure from binaries, clusters and associations, and from large scale tidal streams ripped from past and present dwarf galaxy satellites of the Milky Way. At mid- to far-IR wavelengths, stellar emission is minimized by virtue of being far out on the Rayleigh–Jeans tail of the stellar spectrum (apart from certain rare classes of dusty stars). At near-IR wavelengths stellar emission is important, but with sufficient sensitivity and angular resolution most Galactic stellar emission, and related structure, can be resolved and removed. IR emission from the ISM (cirrus) is intrinsically diffuse and cannot be resolved. Cirrus emission is known to extend to wavelengths as short as 3 μm. Statistically, the structure of the

cirrus emission can be modeled with power–law distributions. Using the mean cirrus spectrum, measurements made in the far-IR can be scaled to 3.5 μm, providing the estimated fluctuation contribution from cirrus that is shown in Figure 5. The extrapolation to shorter wavelengths is highly uncertain, because cirrus (diffuse ISM) emission has not been detected at these wavelengths, and the effects of extinction may become more significant than those of emission, but the cirrus contribution is expected to be several orders of magnitude lower than the CIB fluctuations.

The current detections of CIB anisotropies from DIRBE and 2MASS are above all these foregrounds. The level of anisotropy compares favorably with theoretical expectations and may indeed contain a significant signal from Population III stars. However, the anisotropy may also contain contributions from galaxies made up of Populations II and I stars, which may be significant and uncertain at high z because of unknown evolution effects. Hence it is important to be able to remove galaxy contribution in future measurements. Galaxies with normal stellar populations fainter than $K \sim 24$ contribute little to the CIB. At fainter magnitudes (and larger redshifts) the emission is likely to be dominated by Population III stellar populations and protogalaxies. Because each unit mass of Population III emits a factor of $\sim 10^5$ more light that the normal (Population I, II) stellar populations, the diffuse flux from (massive) Population III stars would dominate emission from faint normal galaxies (say $K \gtrsim 24$). The figure shows that CIB fluctuations from Population III would be the dominant source of diffuse light fluctuations on arcminute and degree scales even if Population III stars epoch was briefer, and their diffuse flux smaller, than the current CIB numbers suggest. Their angular power spectrum should be very different from other sources of diffuse emission and its measurement thus presents a way to actually discover Population III and measure the duration of their era and their spatial distribution. The latter would provide direct information on primordial power spectrum on scales and at epochs that are not easily attainable by conventional surveys. This measurement would be imperative to make and is feasible with the present day space technology.

5. Observational requirements

There are several ways in which observations could verify the analysis of this paper. The James Webb Space Telescope (JWST) will be capable of resolving individual Population III objects in their supernova phase, or as young black holes accreting substantial mass flows. Alternatively, if the Population III objects are sufficiently clustered in space and time, the aggregations would resemble proto-galaxies and could be recognized. Observations of these objects are among the foremost objectives of the JWST.

The following would be the optimal set of parameters for an observation designed to map the contribution of the first star era to CIB anisotropies: 1) In order to make certain that the signal is not contaminated by distant galaxies with normal stellar populations, one would need to conduct a deep enough survey in order to identify and eliminate normal galaxies from the field. In practice, as Fig. 1 indicates, going to K$\simeq$ 24 would be sufficient. With the current technology this would take ~ 1.5 hours for a 1 meter space telescope. 2) A direct signature of Population III signal is that there should be no CIB fluctuations at wavelengths $\leq 912(1+z_f)^{-1}$ Å. That spectral drop would provide an indication of the epoch corresponding to the end of first star era. At longer wavelengths the spectral energy distribution of the CIB fluctuations would probe the history of energy emission and its re-distribution by the nearby gas during the first star era. At wavelengths $\gtrsim 10\mu$m zodiacal light fluctuations may become dominant. 3) On angular scales from a few arcminutes to $\sim 10^\circ$ Population III would produce CIB anisotropies with a distinct and measurable angular spectrum, but its measurement will be limited by the cosmic or sampling variance. If the power spectrum is determined from fraction $f_{\rm sky}$ of the sky by sampling in concentric rings of radius $q \sim \pi/\theta$ and width Δq, the relative uncertainty on $P_2(q)$ will be $\sim (2\pi)^{-1}\frac{\theta}{180^\circ}\sqrt{\frac{q}{\Delta q}}\ f_{\rm sky}^{-1/2}$. In order to get accurate and independent measurements, it is necessary to have small $\Delta q/q \sim 0.05-0.1$; thus for reliable results on scales up to θ one would need to cover area a few times larger. Shaded regions in the left panel of Fig. 5 show the one sigma cosmic variance uncertainty with $\Delta q/q = 0.05$ for a total of 1, 100 and 1,000 deg^2 areas covered. In order to get reliable results on scales up to $\theta \gtrsim 1^\circ$ one would need to observe areas of $\gtrsim 10^\circ$ across.

The black box in Fig. 6 shows what parameters the ideal space mission should have for such a measurement with cross-hatched region in the right panel displaying the magnitude range where Population III stars are expected to dominate CIB anisotropies. For comparison other currently operating or planned NASA missions in the near-IR are also shown. Some of the datasets overlap with the required parameter space, but a large part of the desired parameter space can not be reached with these other data sets.

Direct observations of the CIB fluctuations with the needed fidelity and angular range is not easy. The foreground objects (stars and low-redshift galaxies, and the interstellar medium) are bright and abundant. However, they do not have the same spatial and spectral distributions as the predicted CIB fluctuations. The first observational requirement is to measure the fluctuations as a function of spatial scale and wavelength, with sufficient corroborating evidence to show that the fluctuations are not the residual of some foreground process.

The predicted fluctuations turn down at angular scales greater than subtended by the horizon at decoupling seen at the first star era, and this must be verified. Masking out contributions from individual galaxies requires angular resolutions of the order of 1 arcsec and adequate depth to remove galaxies of K $\lesssim 23 - 24$. Observing fluctuations on the order of 3 degrees in size with reasonable resolution of the spatial scale and reasonable signal-to-noise ratio requires a map of the order of 1000 deg^2 in size, about 1/40 of the whole sky. Taken at face value, we need a map of the order of $\simeq 10^{10}$ pixels, to be built up as a mosaic of exposures with individual detectors and telescope pointings.

There are many technical challenges associated with such a project. Ideally the observations would be taken in space, to avoid the limitations of atmospheric noise, and to enable observations at the full range of wavelengths from 1 to 5 μm. In addition, we would require software to stitch together exposures from different detectors, taken at different times with different telescope orientations, and different amounts of zodiacal light and cosmic ray hits on the detectors, while preserving accurate calibration. It is essential to preserve large-scale photometric accuracy to

enable measurements of fluctuations on scales larger than a single field of view (Fixsen et al 2000). To understand and eliminate the effects of interstellar dust and PAH clouds, it will be necessary to provide photometric bands that maximize the detectability of these sources of interference. In addition, observations over wide ranges of foreground brightness would enable recognition of unexpected effects. Such a project would produce a large database of space observations of low-contrast, extended features, and could lead to unexpected discoveries.

To summarize, the measurement of CIB fluctuations from the Population III star era is imperative to make and is feasible with the present day space technology.

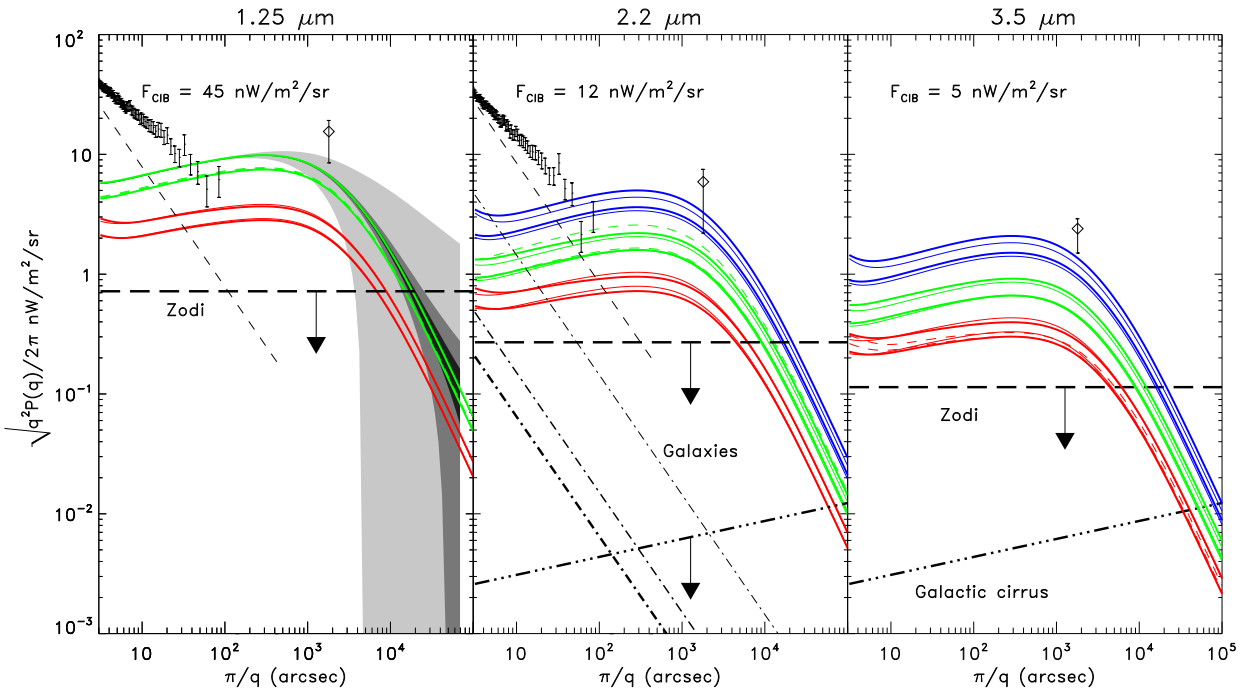

Fig. 5.— CIB fluctuations, $\sqrt{q^2 P_2/2\pi}$, from Population III stars forming at $z_* = 20$. Continuous blue, green and red lines correspond to $z_f = 15, 10, 6$ respectively. Thin colored solid lines correspond to the case of constant CIB flux rate production and b_ν = const. Thick colored solid lines correspond to $dI_\nu/dt \propto f_* b_{\nu'}$ with $b_\nu \propto \nu^2$. Lower lines correspond to $T_{\rm vir} = 400$K, and top lines to $T_{\rm vir} = 2000$K. Colored dashed lines show the CIB fluctuations for more realistic SED from Santos et al (2002) which include the Lyman-α and free-free emission from the surrounding nebula. They mostly overlap with the other SED models showing the relative model-independence of the results. Thin and thick dashed colored lines correspond to SED from Fig. 3 (completely opaque nebula to ionizing photons) and Fig. 5 (completely transparent nebula). Thin dashed lines show atmospheric fluctuations from ground based 2MASS measurements after 1 hour of exposure. Thick long dashes denote the upper limit on zodiacal light fluctuations from Abraham et al 1997 scaled to the corresponding band. Thick dashed-triple-dotted line denotes cirrus fluctuations: these are upper limits at 2.2 micron and an estimate from Kiss et al 2003 at 3.5 micron. In the middle panel dot-dashed lines correspond to shot noise from galaxies fainter than K=24 (thickest), K=23 and K=20 magnitudes (thin). The K-band faint galaxy counts data used were taken from Totani et al 2001. Diamonds with error bars show the CIB fluctuations at $\sim 0.7^\circ$ from the COBE DIRBE fluctuations analysis (Kashlinsky & Odenwald 2000a). Note that because of the large DIRBE beam, the results include contribution from all galaxies as well as other sources such as Population III. Dots with error bars show the K band CIB fluctuation from deep integration 2MASS data (Kashlinsky et al 2002. The 2MASS data shown in the figure were taken for the the patches for which galaxies were removed brighter than $K \simeq 19^m$ (Odenwald et al 2003). The cosmic variance 1-sigma uncertainty is shown with shaded regions in the left panel. The darkest shade corresponds to a total of 1,000 deg^2 observed, the intermediate shade corresponds to a total of 100 deg^2 and the lightest shade corresponds to 1 deg^2.

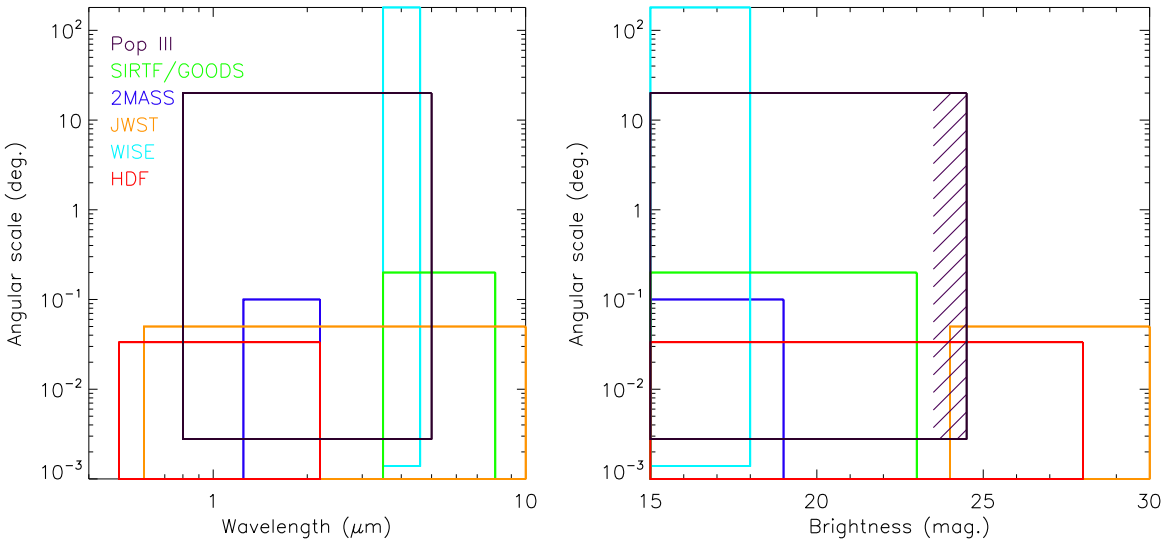

Fig. 6.— Black rectangular box shows the regions of the parameters for a mission to measure the CIB anisotropies from Population III thereby detecting the first star era. Cross-hatched region in the right panel displays the magnitude range where Population III stars are expected to dominate CIB anisotropies.Other colors correspond to the currently existing datasets or planned NASA missions useful for this purpose: red is the Hubble Deep Field from HST (http://www.stsci.edu/ftp/science/hdf/hdf.html), dark blue is for the deep 2MASS data (Kashlinsky et al 2002, Odenwald et al 2003), green is the NASA SIRTF GOODS project (http://www.stsci.edu/ftp/science/goods/), light blue corresponds to the planned NASA WISE MIDEX mission (http://www.astro.ucla.edu∼wright/WISE), and orange color corresponds to the field-of-view of the NASA James Webb Space Telescope planned for the end of the decade (http://jwst.gsfc.nasa.gov).

REFERENCES

Abel, T. et al 2002, Science, 295, 93

Ábrahám, P., Leinert, Ch., & Lemke, D. 1997, A&A, 382, 702-705

Baraffe, L, Heger, A. & Woosley, S.E. 2001, Ap.J.,550,890

Bennett, C. L. et al 2003,Ap.J.Suppl.,148,1

Bond, J.R., Arnett, W.D. & Carr, B.J. 1984,Ap.J.,280,825

Bond, J.R., Carr, B.J. & Hogan, C. Ap.J., 1986,306,428

Bromm, V. et al 1999, Ap.J., 527, L5

Cambresy, L. et al 2001,Ap.J.,555,563

Cooray, A. et al 2003, astro-ph/0308407

Dwek, E. & Arendt, R. 1998, Ap.J.,508,L9

Fixsen, D. J., Moseley, S. H., Arendt, R. G. 2000, Ap.J.Supp., 128, 651

Gardner, J.P. 1996,in "Unveiling the cosmic infrared background", ed. E. Dwek, p. 127

Gorjian, V. et al 2001,536,550

Hauser, M. et al 1998, Ap.J.,508,25

Hauser, M. & Dwek, E. 2001, Ann Rev A A, 39, 249

Jensen, L. & Szalay, A., 1986, Ap.J.,305,L5

Jimenez, R. & Kashlinsky, A. 1999, Ap.J.,511,16

Kaiser, N. 1984, Ap.J.,284,L9

Kashlinsky, A. 1987, Ap.J.,317,19

Kashlinsky, A. 1998, Ap.J.,492,1

Kashlinsky, A., Mather, J.C., Odenwald, S. & Hauser, M. 1996, Ap.J.,470,681

Kashlinsky, A., Mather, J.C., Odenwald, S. 1999, preprint

Kashlinsky, A. & Odenwald, S. 2000a, Ap.J.,528,74

Kashlinsky, A. & Odenwald, S. 2000b, Science,289,246

Kashlinsky, A., Odenwald, S., Mather, J.C., Skrutskie, M. 2002, Ap.J,579,L53

Kiss, Cs., et al 2003, A&A, 399, 177-185

Kogut, A. et al 2003, Ap.J.Suppl.,148,161

Madau, P. & Pozzetti, L. 2000,MNRAS,312,L9

Magliochetti, M., Salvaterra, R., Ferrara, A. 2003, MNRAS,342,L25

Matsumoto, M. et al 2000,in "ISO surveys of a dusty Universe", eds. Lemke, D. et al. p.96

Miralda-Escude, J. 2003, Science, 300, 1904

Odenwald, S., Kashlinsky, A., Mather, J.C., Skrutskie, M. 2003, Ap.J,583,535

Peacock, J.A. & Dodds, S.J., 1996, MNRAS,280,L19

Politzer, H.D. & Wise, M.B. 1984, Ap.J.,285,L1

Press, W. & Schechter, P. 1974, Ap.J., 187, 425

Rees, M.J. 1978, Nature,275,35

Salvaterra, R. & Ferrara, A. 2003, MNRAS,339,973

Santos, M.R., Bromm, V., Kamionkowski, M. 2002,MNRAS,336,1082

Schaerer, D. 2002, Aston. Astrophys., 382,28

Schneider, S. et al 2002,Ap.J.,571,30

Totani, T. et al 2001,Ap.J.,559,592

Tumlinson, J., Shull, J.M., & Venkatesan, A. 2003,Ap.J.,584,608

Wright, E.L. 2003,astro-ph/0306058

Xu, J. et al 2002, Ap.J., 580, 653

Yoshii, Y. & Peterson, B. 1994, Ap.J.,436,551